PERGAMON

Deep-Sea Research I 45 (1998) 1577–1593

DEEP-SEA RESEARCH
PART I

Patterns in the size structure of the phytoplankton community in the deep fluorescence maximum of the Alboran Sea (southwestern Mediterranean)

Jaime Rodríguez[a,*], José M Blanco[a], Francisco Jiménez-Gómez[a], Fidel Echevarría[b], Julio Gil[c], Valeriano Rodríguez[a], Javier Ruiz[b], Begoña Bautista[a], Francisco Guerrero[a]

[a] *Departamento de Ecología, Facultad de Ciencias, Universidad de Málaga, 29071-Málaga, Spain*
[b] *Facultad de Ciencias del Mar, Universidad de Cádiz, Spain*
[c] *Centro Oceanográfico de Santander, Instituto Español de Oceanografía, Santander, Spain*

Received 9 January 1997; received in revised form 20 June 1997; accepted 21 November 1997

Abstract

The Alboran Sea (southwestern Mediterranean) exhibits strong horizontal and vertical gradients associated with macroscale and mesoscale physical structures due to the input of surface Atlantic waters into the Mediterranean basin. During the summer of 1992, two anticyclonic and two cyclonic areas were found with fluorescence maxima (DFM) below the seasonal thermocline (ST). Although the depth of the ST is fairly constant, the position and intensity of the DFM is more variable, with a tendency to deepening and smoothing in the anticyclonic gyres. The position of the Atlantic–Mediterranean interface (AMI) can be used as a tracer for cyclonic or anticyclonic dynamics and their *potential* biological effects. A shallow AMI indicates divergence or upwelling dynamics and coincides with the highest fluorescence intensity, chlorophyll concentration and phytoplankton biovolume in the DFM. Under the conditions typical of the two anticyclonic gyres, the contrary is found. The size structure of phytoplankton shows significant differences between cyclonic and anticyclonic structures. Log-transformed size-abundance spectra can be adequately described by linear models with slopes of -0.78 for cyclonic and -0.93 for anticyclonic structures. The integration of size-abundance spectra indicates that picoplankton biovolume in the DFM is independent of the type of circulation or dynamics, whereas nanoplankton and, particularly, microplankton increase their absolute and relative presence in the DFM under cyclonic or upwelling dynamics.

* Corresponding author. E-mail: jaime@ums.es

0967-0637/98/$–see front matter
PII: S0967-0637(98)00030-2

1. Introduction

The presence of a deep or subsurface chlorophyll maximum (DCM) is a common feature of profiles collected from the oligotrophic oceanic gyres or during summer in temperate seas (Herbland and Voituriez, 1979; Cullen, 1982; Longhurst and Harrison, 1989; Mann and Lazier, 1991; Estrada *et al.*, 1993; Li, 1994). The mechanisms and processes that control the origin and position of the DCM differ widely (see Cullen, 1982; Longhurst and Harrison, 1989; Varela *et al.*, 1992, 1994; Ruiz *et al.*, 1996). Where sinking and accumulation are the main formation mechanisms, phytoplankton at the DCM is expected to show a composition similar to that in the surface layer. If the DCM is mainly explained by the *in situ* growth of cells adapted to low light conditions, then taxonomical and other differences can appear between layers (see Venrick *et al.*, 1973; Beers *et al.*, 1975; Furuya and Marumo, 1983; Latasa *et al.*, 1992 as examples of different cases).

Under oligotrophic, open ocean conditions the DCM is usually deeper and has lower chlorophyll concentration than under more productive conditions (Li, 1994). In the first case, where photoadaptation can be expected to be relevant, small cells typically <3 μm usually dominate the DCM environment due to their better efficiency at low light levels (Bienfang and Szyper, 1981; Li and Wood, 1988; Platt *et al.*, 1983). This is consistent with the results of Ruiz *et al.* (1996), who found that the slope of the size-abundance spectrum of phytoplankton (Platt and Denman, 1977, 1978; Sprules and Munawar, 1986; Rodríguez and Mullin, 1986) is more negative at the level of the DCM, indicating a higher proportion of small cells in the DCM as the result of favourable light-limited growth conditions.

What can we expect about the size structure of phytoplankton when the DCM is shallower and encloses high chlorophyll concentration, as is the case under upwelling or more productive conditions? Observations of Malone (1971, 1980), Margalef (1978), models such as those proposed by Legendre and Le Fèvre (1989) and the more recent data compilation of Chisholm (1992) suggest that large phytoplankton should characterize these areas, but a precise analysis of the size structure of the complete phytoplanktonic community is still lacking.

The Alboran Sea (southwestern Mediterranean) offers a unique opportunity to study the variability of the size structure of the phytoplankton community in the DCM layer, due to the close presence of anticyclonic (oligotrophic) and cyclonic (productive) gyres resulting basically from the interchange of water between the Atlantic and the Mediterranean through the Gibraltar Strait (Lacombe, 1971; Lanoix, 1974; Cano, 1978; Lacombe and Richez, 1982; Parrilla and Kinder, 1987; Gascard and Richez, 1985; Tintoré *et al.*, 1991). During summer stratification, in those zones with a two-layered system formed by surface modified Atlantic waters over Mediterranean waters, there is a salinity interface and pycnocline, usually deeper than the seasonal thermocline. In the horizontal plane, the interaction between the Atlantic and Mediterranean waters determines the proximity of diverse structures such as cyclonic and anticyclonic gyres, fronts and upwelling phenomena with characteristic mesoscale and macroscale dimensions (see Tintoré *et al.*, 1991). This makes the Alboran Sea a natural laboratory to analyze the variability of DCM characteristics under

different physical conditions and for the study of physical and biological interactions in the ocean.

In this paper we compare several properties of the phytoplankton community in the deep fluorescence maximum of the Alboran Sea. The position, fluorescence intensity, chlorophyll content, phytoplankton biovolume and size-spectrum model parameters in the DFM are related to the cyclonic or anticyclonic character of the gyres.

2. Methods

2.1. Field measurements

The "Ictio-Alborán 92" cruise (11–25 July 1992) of the R.V. "F.P. Navarro" occupied 51 stations (Fig. 1). Continuous vertical profiles of temperature, salinity and depth were made in the upper 200 m with a Sea-Bird 25 CTD equipped with a Sea Tech fluorometer. From these vertical profiles three basic attributes were defined:

"DFM depth": the depth of the peak of the fluorescence profile. CTD readings were averaged to give values every 1 m depth. A few profiles presented a second, less pronounced and deeper peak; the maximum fluorescence value was always selected to define DFM depth.

"ST depth": the depth of the bottom of the highest temperature gradient. For each sampling station, gradients were measured every 5 m depth for series 0–5, 1–6, 2–7 m and so on in an iterative process. Once the layer with the highest gradient was

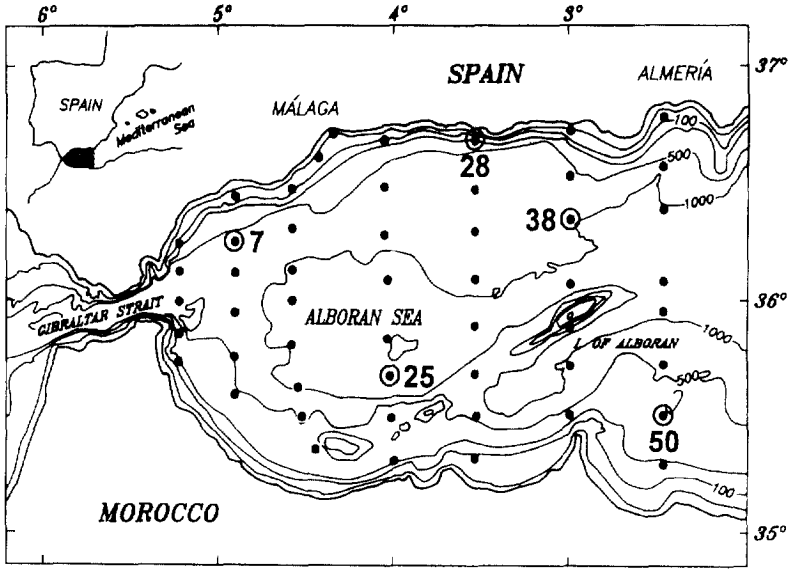

Fig. 1. Area of study and sampling stations. The positions of stations representative of either cyclonic or anticyclonic structures (7, 38, 25, 50) or typically Mediterranean character (28) are indicated.

identified, the depth corresponding to the bottom of the layer was selected. Obviously, describing the location of the thermocline as a single depth is a crude simplification, but the only aim was to have a value comparable to "DFM depth".

"AMI depth": the depth of the 37.5 salinity value. In fact this is the bottom of the AMI interface layer defined by Lacombe and Richez (1982) as the layer between 37.0 and 37.5.

At each station, seawater samples were taken with Niskin bottles at 0, 20, 100 m, the depth of the DFM and three other varying depths around the DFM. Water samples were filtered through Whatman GFF filters, and pigments were extracted with 90% acetone for 24 h in the dark in a cold chamber. Chlorophyll concentration was determined with a Turner Designs fluorometer.

The size distribution of phytoplankton abundance was analyzed on samples from the DFM layer through a combination of flow cytometry and microscopy-image analysis. Following the procedure recommended by Vaulot *et al.* (1989), 10 ml samples were preserved with 1% glutaraldehyde and stored in liquid nitrogen for flow cytometric (FC) analysis. An additional 100 ml was preserved with lugol for microscopy analysis.

2.2. *Flow cytometry analysis*

In the laboratory, FC samples were filtered through a 40 μm net and analysed with a FACScan (Becton Dickinson) flow cytometer with the following acquisition parameter settings: FSC = E00; SSC = 271; FL1 = 450; FL2 = 450; FL3 = 300 and a threshold for chlorophyll fluorescence (FL3) = 001. Sample volume was deduced from the time of analysis (500 s) and the flow rate ("high" setting = 60 μl min^{-1}). Data were acquired in "list mode" and processed with the help of Lysis II software. The smallest cells identified and adequately quantified with these settings are cyanobacteria (*Synechococcus*). We did not run a second analysis for very small prochlorophytes, whose contribution to the size-abundance spectra has yet to be studied in these waters.

2.3. *Microscopy and image analysis*

After sedimentation of the Lugol's preserved sample, cells and colonies were counted and measured at 100× and 200× in a Nikon TM2 inverted microscope connected to a VIDS-IV (Analytical Measuring Systems) semi-automatic image analysis system, following the protocols in Echevarría and Rodríguez (1994) and Ruiz *et al.* (1996).

2.4. *Calibration and preservation tests*

Prior to sample analysis, the light scattering signal of the flow cytometer was calibrated against image-analysis volume measurements of the following cell cultures: *Synechococcus* sp. (around 1 μm), *Nannochloris atomus* (2–4 μm), *Nannochloropsis gaditana* (2–5 μm), *Isochrysis galbana* (3–5 μm), *Phaeodactylum tricornutum* (3–6 μm) and *Tetraselmis chui* (8–11 μm), whose flowcytometric identification appears in Fig. 2A.

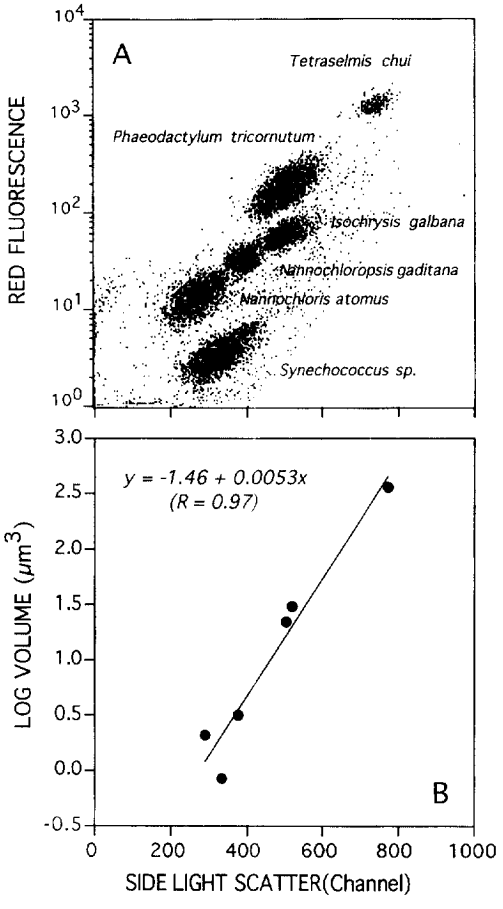

Fig. 2. (A) Flow cytometry discrimination of the six cultured species employed in the calibration of light scatter signal. (B) Relationship between side scatter channel and cell volume for the cultured phytoplankton populations.

Population size structure was analysed with the VIDS-IV video-interactive image analysis system described previously. The relation between side light scatter (SSC) and cell volume for these species appears in Fig. 2B, together with the equation employed to transform SSC channel to size (volume) equivalent. Although preservation followed recommendations of Vaulot *et al.* (1989), we tested this effect under our particular working conditions. There were no apparent differences in the flow cytometric features of populations between fresh and preserved samples.

2.5. Size spectrum analysis

The coupling of flow cytometry and image analysis analytical subranges produces a size ($\log_2$ volume scale)-abundance spectrum of phytoplankton that adequately

covers the ensemble from picoplankton to microplankton. The flow cytometry covers approximately the subrange from 0.5 μm Equivalent Sphaerical Diameter (the lower limit of the volume class between 0.125 and 0.256 μm^3) to 13 μm (the upper limit of the volume class between 512 and 1024 μm^3). The image analysis subrange is from about 8 μm (the lower limit of the 256–512 μm^3 volume class) to 80 μm (the upper limit of the volume class between 1.3×10^5 and 2.6×10^5 μm^3). Both subranges are conservative in the sense that size classes of very small or very large cells, potentially underestimated, were eliminated for size spectrum statistical analysis (see García *et al.*, 1994).

A linear model can be fitted to the spectrum with the aim of examining the relation between model parameters and the physical environment (Rodríguez, 1994; Echevarría and Rodríguez, 1994; García *et al.*, 1994). The empirical size-abundance spectrum also allows determination of total biovolume (μm^3/ml) for a particular size compartment (for example, nanoplankton, covering size classes between 2 and 20 μm) as

$$B = \sum_i n_i v_i,$$

where n_i is the number of cells in the size class i with nominal volume v_i. In this study, nominal volume is the lower limit of a particular class (but see Blanco *et al.*, 1994, for other possibilities).

3. Results and discussion

3.1. Physical background

Fig. 3 describes the main hydrodynamical features found during the study. The Atlantic jet feeds the permanent, macroscale southwestern anticyclonic gyre (A1, see references above) and a second, smaller and less persistent anticyclonic gyre (A2) to the east of the Tres Forcas Cape (see Tintoré *et al.*, 1991). Between these two structures a cyclonic eddy occupying the central-eastern part of the basin (C2) is similar to the one described by Tintoré *et al.* (1991). Another cyclonic area (C1), north of the large-scale structure A1, affects the northwestern Alboran Sea between the Gibraltar Strait and the bay of Málaga; this is usually related to upwelling phenomena in the area (Cano, 1978; Gil and Gomis, 1994).

These four structures are represented by the T–S diagrams in Fig. 4. The water column of station 25, situated in the core of A1, has a layer of modified Atlantic surface water (ASW, 36.5 salinity) over the layer of deep Mediterranean waters (DMW, >37.5). The Atlantic surface water is warmer and its salinity higher at station 50, where the current forms the second anticyclonic gyre (A2). Both cyclonic gyres C1 and C2 (represented by stations 7 and 38, respectively) have a surface layer of Atlantic modified water with salinity signatures very similar to that found in A2 but lower surface temperatures, particularly C1. Fig. 4 also includes the T–S profile

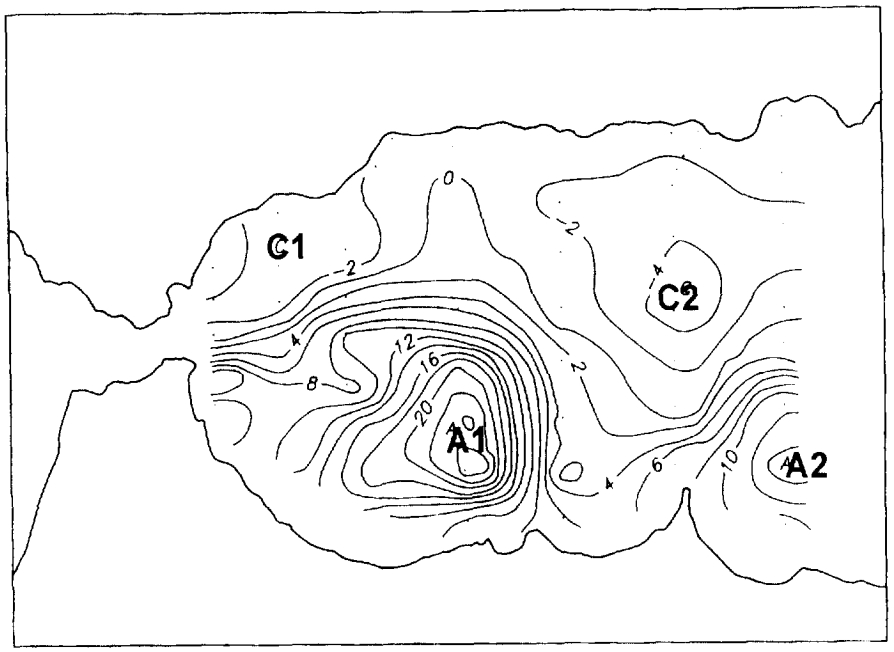

Fig. 3. Dynamical topography (200 mb reference level) of the studied area. C1, C2, A1 and A2 represent the nuclei of cyclonic and anticyclonic structures.

corresponding to station 28 (see Fig. 1), where the surface layer of Atlantic modified water is no longer present. Here, instead of the layered system formed by ASW–AMI–DMW, we found a continuous transition from surface to deep Mediterranean water types. This situation is typical of some stations in the northeast coastal sector of the basin (Cano *et al.*, 1997).

3.2. Relations between DFM, ST and AMI

The depth of the ST (see Methods) is quite constant at the whole basin scale (mean = 21.3 m; s.d. = 6.5), as it is the depth of the main associated seasonal pycnocline (Fig. 5). There is a clear difference between the density gradient in C2 (but not in C1) and the two anticyclonic gyres. On the other extreme, the AMI depth (S = 37.5, see Section 2) is highly variable. It ranges from 36 to 178 m and lies below 100 m in the two anticyclonic gyres (Fig. 5, A1 and A2). It is shallower in the cyclonic areas, where it can be very close to the seasonal thermocline or pycnocline (Fig. 5, C2).

The depth of the DFM shows intermediate variability. It ranges from 17 to 71 m (mean = 45 m; s.d. = 13.9). The deepest (60–70 m) location and lowest fluorescence intensity were found in the two anticyclonic gyres (Fig. 5, A1 and A2), in agreement with the accumulation of surface water and consequent oligotrophy. Here, chlorophyll concentration in the DFM is 1 $\mu g l^{-1}$. The DFM is shallower (30–40 m) in the

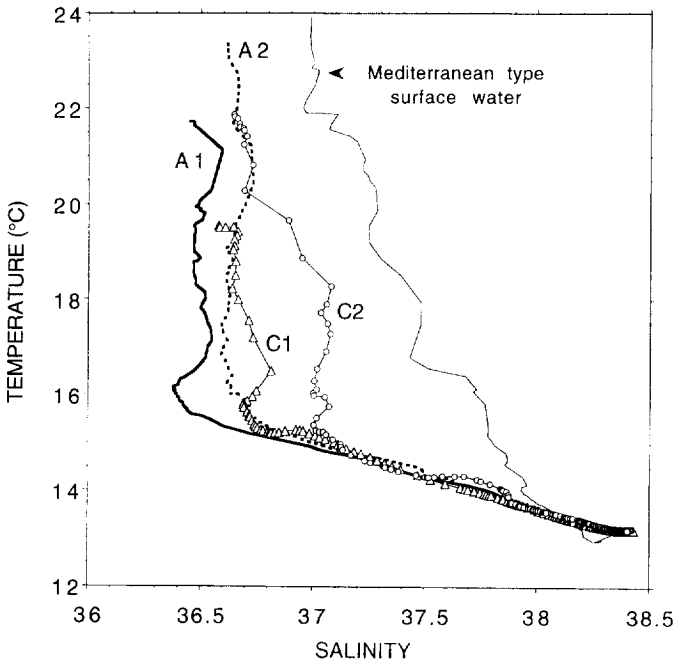

Fig. 4. Temperature–salinity diagrams of some stations representative of cyclonic (C1, C2) and anticyclonic (A1, A2) structures. Station 28, with Mediterranean-type surface water, is also shown for comparison.

cyclonic areas (Fig. 5, C1 and C2), in accordance with the divergence pattern and upwelling that usually characterize these structures. Fluorescence intensity and chlorophyll concentration in the DFM increase by more than a factor of 2 between C1 (3.1 μg chlorophyll l^{-1}) and C2 (7.4 μg chlorophyll l^{-1}).

In all cases the DFM is below the ST (Fig. 5). This finding agrees with the generalization of Longhurst and Harrison (1989) for a seasonally stabilising water column, with the DCM trapped below the thermocline at the bottom of the euphotic zone. A similar relative position for the DCM has been described by Estrada *et al.* (1993) in northwestern Mediterranean waters.

On the other hand, Fig. 6 suggests that there is an inverse relation between AMI depth and the *maximum* value of any of the two indicators of phytoplankton abundance (fluorescence intensity and chlorophyll concentration) in the DFM. Under anticyclonic circulation, the AMI goes below 100 m depth, with a clear decreasing tendency of the maximum chlorophyll concentration in the DFM, in correspondence with the oligotrophic conditions determined by this type of vertical motion. Under cyclonic circulation the AMI can be found at around 40 m depth. In these cases, chlorophyll concentration in the DFM can reach maximum concentrations close to 8 μg l^{-1}, although actual values are highly variable (Fig. 6). Our interpretation is that a shallow AMI indicates only the necessary conditions for nutrient availability and

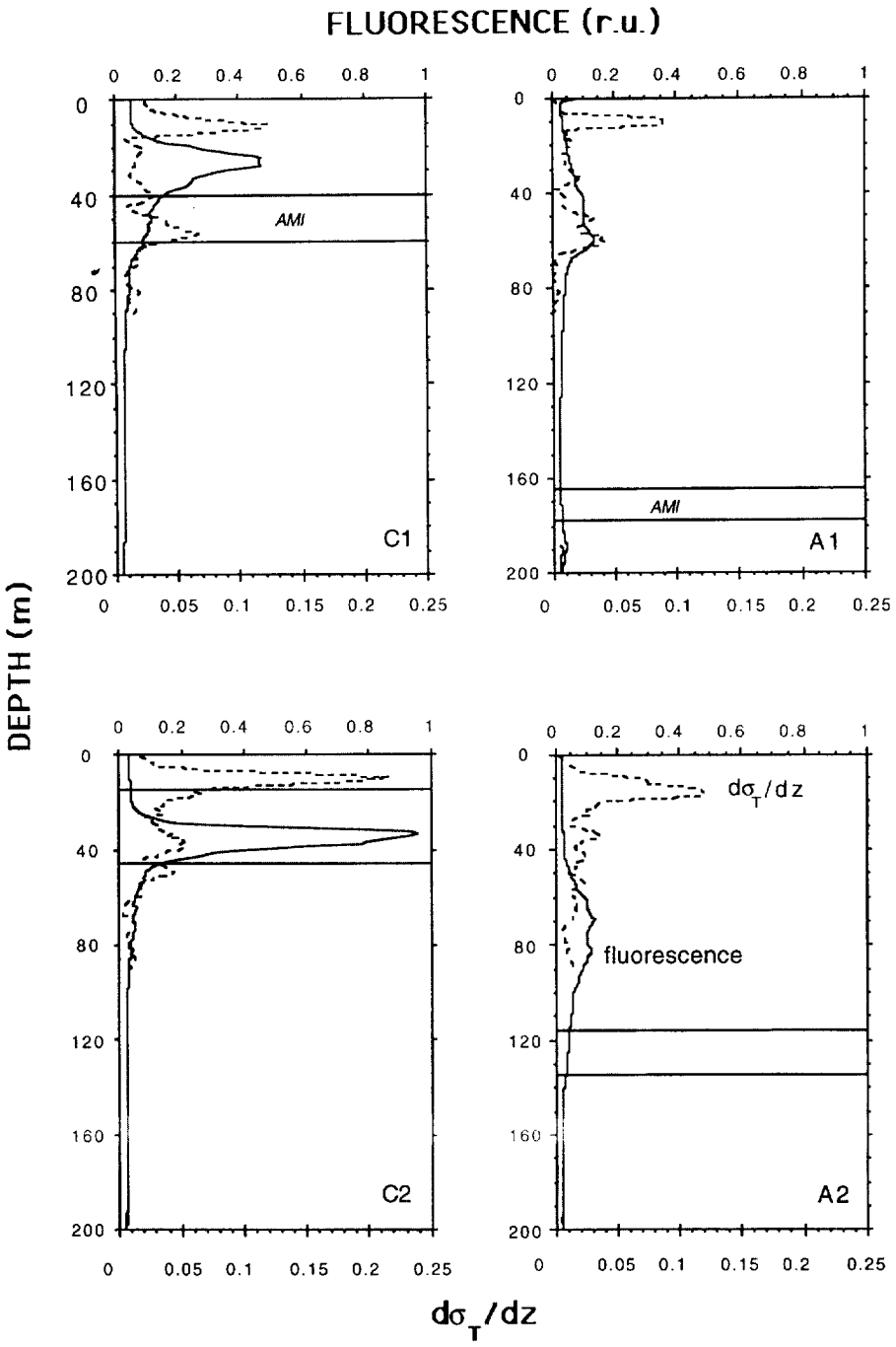

Fig. 5. Vertical profiles of $d\sigma_t/dz$ and fluorescence in the four selected structures. The Atlantic–Mediterranean Interface (AMI) is also shown as a layer of variable depth and width.

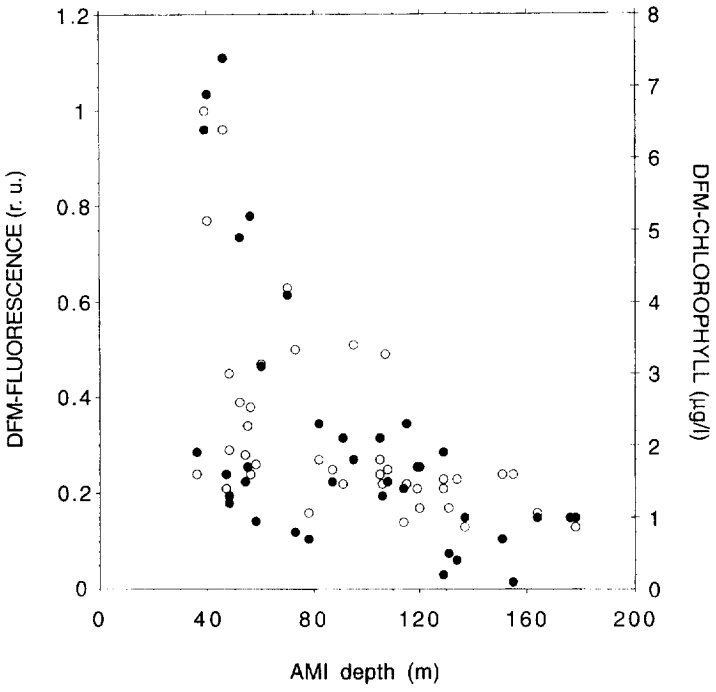

Fig. 6. Relation between AMI depth, DFM fluorescence intensity (○) and chlorophyll concentration (●).

phytoplankton growth, but there are additional factors, like grazing or sinking, that can control phytoplankton biomass accumulation in the DFM. All these processes operate at time scales that could be partially uncoupled from the space and time scales of our observations, thus producing the variability of observed chlorophyll measurements under conditions potentially favourable for phytoplankton growth. Thus we conclude that AMI depth can be used as a tracer for cyclonic or anticyclonic dynamics and their potential biological effects, indicated by the maximum values that DFM chlorophyll concentration can reach.

3.3. Size structure of phytoplankton

It is an accepted idea that phytoplankton in the open ocean is dominated by small cells (picoplankton), whereas coastal and productive areas are dominated by large cells ("net-plankton") (Malone, 1971). Similar changes are also described along the succession process from the mixed, nutrient-rich waters, which favour the development of a diatom spring bloom, to the oligotrophic conditions found in the upper water column at the end of the summer stratification period, which favour the dominance of small flagellates with a high affinity for regenerated nutrients (Margalef, 1978; Legendre and Le Fèvre, 1989).

The majority of studies addressing the size structure of phytoplankton biomass rely on measurements of size-fractionated chlorophyll (Takahashi and Bienfang, 1983; Peña *et al.*, 1990; Rodríguez and Guerrero, 1994). This approach, in spite of its many technical and interpretative inconveniences, supports the generalization that the open, oligotrophic ocean is characterized by picoplankton whereas coastal, productive areas permit the development of large-cell phytoplankton populations. Harris *et al.* (1987) found that, over the year in Tasmanian waters, there is a relationship between the chlorophyll content of surface waters and the slope of the log–log plot of the size–density spectrum. According to these authors (see also Chisholm, 1992, for a review) high chlorophyll values arose only from the presence of large phytoplankton, which results in less negative values of the spectrum slope. Sprules and Munawar (1986) had previously shown that the slope of the size-abundance spectrum becomes less negative as ecosystem eutrophy increases. They compare the complete planktonic spectra (phytoplankton + zooplankton) from many lakes and include the oligotrophic ocean case from Rodriguez and Mullin (1986). Their explanation is that the higher turnover rate of phytoplankton in eutrophic ecosystems enables a higher biomass of zooplankton to be sustained.

The size distribution of phytoplankton abundance in the four cases we have selected previously (Fig. 7) is characterised by a good linear relation between the log-transformed values of cell abundance and size (Table 1). This is in agreement with

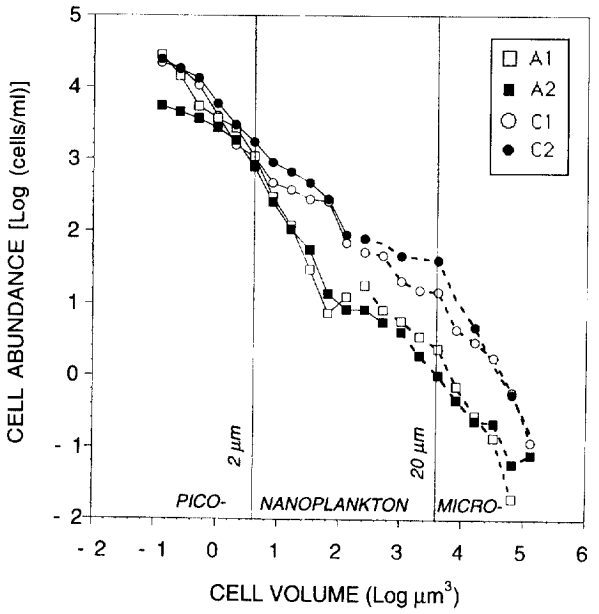

Fig. 7. Phytoplankton size-abundance spectra in the DFM of the four selected structures. Continuous line: flow cytometry subrange; broken line: image analysis subrange.

Table 1
Parameter values and regression coefficients of the size-abundance spectra model log [cell abundance (cells/ml)] = $a - b$ log [cell volume (μm^{-3})] for selected stations placed within the core of cyclonic (C) and anticyclonic (A) structures as well as their combination

Structure (St. no.)	$a \pm 95\%$ c. l.	$b \pm 95\%$ c. l.	r^2	p
A1 (25)	3.46 ± 0.22	-0.97 ± 0.08	0.97	<0.0001
A2 (50)	3.14 ± 0.17	-0.89 ± 0.06	0.98	<0.0001
C1 (7)	3.63 ± 0.14	-0.79 ± 0.05	0.98	<0.0001
C2 (38)	3.78 ± 0.20	-0.77 ± 0.07	0.96	<0.0001
A1 + A2	3.30 ± 0.14	-0.93 ± 0.05	0.97	<0.0001
C1 + C2	3.71 ± 0.12	-0.78 ± 0.04	0.97	<0.0001

theoretical predictions (Sheldon *et al.*, 1972; Platt and Denman, 1978) and empirical observations in the ocean (Platt *et al.*, 1984; Rodríguez and Mullin, 1986). However, slope values range from -1.0 to -0.65 (mean $= -0.85$, s.d. $= 0.10$), which, in general, are less negative than those predicted by theoretical methods (-1.20 to -1.0) or measured in the ocean (-1.16) by the above cited authors. It is important, however, not to forget that our size-abundance spectra refer exclusively to the autotrophic component of the planktonic community. In any case, it is useless to look for a common, universal slope value with a unique explanation (see Rodríguez, 1994 for a review) simply because of the highly different size ranges and methodologies described by different authors. The important fact is that, frequently, the size spectrum can be described by a simple log-linear model, that can be used as a tool in the analysis of spatial and temporal variability of the pelagic ecosystem (Platt *et al.*, 1984; Chisholm, 1992; Rodríguez, 1994). In this context, our results indicate that the size spectrum in cyclonic areas of the Alborán Sea has a slope less negative (-0.78 ± 0.04, Table 1) than the spectrum in the anticyclonic areas (-0.93 ± 0.05, Table 1). An ANCOVA analysis (Sokal and Rohlf, 1995) of the four spectra shows no significant differences among the means of the distributions ($p > 0.28$). However, differences are significative among slopes ($p < 0.0001$) as well as among intercepts ($p < 0.0001$), thus supporting the conclusion that the size distributions in cyclonic and anticyclonic gyres are significatively different.

Differences between spectra seem to be minor in the picoplankton size range (Fig. 7) and increase within the nanoplankton compartment up to a maximum difference in the limit between nanoplankton and microplankton. The size spectrum of C2 shows a change in slope just in the transition from flow cytometry to image analysis subrange, which in principle might be considered an artifact. However, Fig. 7 shows that, with the same methodologies, there is no slope change in C1 and A2 cases. In fact, the change in slope observed in C2 is explained by the accumulation of diatoms (*Rhizosolenia* spp.) in the DFM. These cells have a characteristic volume between 4000 and 8000 μm^3 (that is, between 20 and 25 μm approximately) and contribute significatively to the high amount of chlorophyll and biovolume in the microplankton

compartment. The size spectrum of A1 also shows a discontinuity just in the transition from flow cytometry to image analysis. In this case, the jump is explained by the accumulation in the DFM of a diverse and relatively abundant community of small dinoflagellates with cell size around 8–10 μm, just in the upper limit of the selected flow cytometry subrange and the first size classes covered by microscopy and image analysis. The conservative character of the subranges selected from each methodological approach allow the conclusion that these are real deviations within the global size spectrum and that they are not artifacts derived from the necessary use of two complementary methodologies.

The approximate constancy and ubiquity of picoplankton is confirmed in Fig. 8, where the biovolume of typical size compartments (as defined by Sieburth *et al.*, 1978) are compared (see Section 2). Biovolume differences between anticyclonic and cyclonic areas are due to nanoplankton and particularly microplankton. Obviously, in terms of cell numbers oligotrophic environments are characterized by the dominance of picoplankton cells, but their absolute contribution to the DFM phytoplankton community does not vary much in spite of the greatly varying physical conditions found in the Alborán Sea. In terms of biovolume, picoplankton abundance is between 20,000 (A1) and 40,000 $\mu m^3 ml^{-1}$ (C2) whereas total biovolume changes

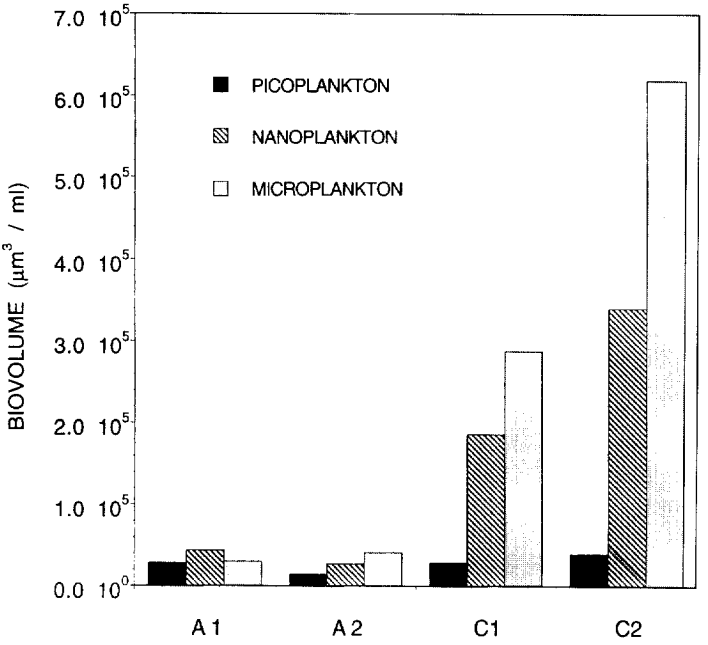

Fig. 8. Comparative integrated biovolume of picoplankton (from 0.6 to 2 μm ESD), nanoplankton (2–20 μm) and microplankton (from 20 μm up to the largest size included in the spectrum, 80 μm) in the four selected structures.

from 10^5 to 10^6 $\mu m^3 ml^{-1}$. Microplankton biovolume is in the same order of magnitude as picoplankton in the anticyclonic gyres but increases sharply up to more than 6×10^5 $\mu m^3 ml^{-1}$ in the cyclonic gyre C2. The nanoplankton compartment follows the same tendency, with intermediate biovolume values. In relative terms, the picoplankton compartment represents approximately $\frac{1}{4}$ of total biovolume in A1 but drops to less than 5% in C2, where microplankton increases up to more than 60% of total biovolume. Nanoplankton relative contribution is rather constant and around 35% of total biovolume in the four cases studied. Thus, picoplankton cells are ubiquitous and their absolute abundance similar under different hydrographic structures. It is the growth and accumulation of large cells (large nanoplankton and mainly microplankton) that make cyclonic gyres different.

Our overall conclusion is that the DFM is shallower in cyclonic areas and contains high chlorophyll and biomass due to the abundance of large cells, which leads to a size-abundance spectrum with a less negative slope. In anticyclonic areas the DFM is deeper and contains low amounts of chlorophyll and biomass due to the absence of large cells, which leads to a more negative slope of the phytoplankton size-abundance spectrum. Picoplankton, or very small cells in general, are invariant in relation to the physical structure at the scales of the study.

Acknowledgements

This study was financed by the Spanish CICYT, Projects MAR91-0813 and AMB93-0614. It was also supported by a Collaboration with the Instituto Español de Oceanografía (IEO). We thank the crew of the R.V. "Francisco de Paula Navarro" for their willingness during the cruise. We also thank Dr Luis Lubián (Instituto de Ciencias Marinas de Andalucía, Spain) for providing cell cultures.

References

Beers, J.R., Reid, F.M.H., Steward, G.L., 1975. Microplankton of the North Pacific Central Gyre. Population structure and abundance, june 1973. Internationale Revue der gesamten Hydrobiologie 60, 607–638.

Bienfang, P.K., Szyper, J.P., 1981. Phytoplankton dynamics in the subtropical Pacific Ocean of Hawaii. Deep-Sea Research 28, 981–1000.

Blanco, J.M., Echevarria, F., García, C.M., 1994. Dealing with size- spectra: some conceptual and mathematical problems. In: Rodríguez, J., Li, W.K.W. (Eds.), The Size Structure and Metabolism of the Pelagic Ecosystem, Scientia Marina, vol. 58, pp. 17–29.

Cano, N., 1978. Resultados de la campaña "Alborán-76". Boletín del Instituto Español de Oceanografía 247, 3–50.

Cano, N., García Lafuente, J., Hernández-Guerra, A., Blanco, J.M., Escánez, J., 1997. Hidrología del Mar de Alborán en Julio de 1993. In: Rubín, J.P. (Ed.), Influencia de los procesos físico-químicos y biológicos en la composición y distribución del ictioplancton estival en el Mar de Alborán y Estrecho de Gibraltar, Informes Técnicos del Instituto Español de Oceanografía 24, 9–26.

Chisholm, S.W., 1992. Phytoplankton size. In: Falkowski, P.G., Woodhead, A.D. (Eds.), Primary Productivity and Biochemical Cycles in the Sea. Plenum, New York. pp. 213–237.

Cullen, J.J., 1982. The deep chlorophyll maximum: comparing vertical profiles of chlorophyll a. Canadian Journal of Fisheries and Aquatic Sciences 39, 791–803.

Echevarría, F., Rodríguez, J., 1994. The size structure of plankton during a deep bloom in a stratified reservoir. Hydrobiologia 284, 113–124.

Estrada, M., Marrasé, C., Latasa, M., Berdalet, E., Delgado, M., Riera, T., 1993. Variability of deep chlorophyll maximum characteristics in the Northwestern Mediterranean. Marine Ecology Progress Series 92, 289–300.

Furuya, K., Marumo, R., 1983. The structure of the phytoplankton community in the subsurface chlorophyll maxima in the western North Pacific Ocean. Journal of Plankton Research 5, 393–406.

García, C.M. et al., 1994. The size structure and functional composition of ultraplankton and nanoplanktont a frontal station in the Alboran Sea. In: Rodríguez, J., Li, W.K.W. (Eds.), The size structure and metabolism of the pelagic ecosystem. Scientia Marina, vol. 58, pp. 43–52.

Gascard, J.C., Richez, C., 1985. Water masses and circulation in the western Alboran Sea and in the Strait of Gibraltar. Progress in Oceanography 15, 157–216.

Gil, J., Gomis, D., 1994. Circulación geostrófica, dinámica de mesoescala y fertilización de aguas someras en el sector norte del Mar de Alborán. Boletín del Instituto Español de Oceanografía 10, 95–117.

Harris, G.P., Ganf, G.G., Thomas, D.P., 1987. Productivity, growth rates and cell size distributions of phytoplankton in the SW Tasman Sea: implications for carbon metabolism in the photic zone. Journal of Plankton Research 9, 1003–1030.

Herbland, A., Voituriez, B., 1979. Hydrological structure analysis for estimating the primary production in the tropical Atlantic Ocean. Journal of Marine Research 37, 87–101.

Lacombe, H., 1971. Le Détroit de Gibraltar. Notes et Mémoires, Service Géologique du Maroc 222, 111–146.

Lacombe, H., Richez, C., 1982. The régime of the Strait of Gibraltar. In: Nihoul, J.C.J. (Ed.), Hydrodynamics of Semi-enclosed Seas. Elsevier, Amsterdam, pp. 13–74.

Lanoix, F., 1974. Project Alboran: Etude hydrologique et dynamique de la mer d'Alboran. NATO Technical Report, 66.

Latasa, M., Estrada, M., Delgado, M., 1992. Plankton-pigment relationships in the Northwestern Mediterranean during stratification. Marine Ecology Progress Series 88, 61–73.

Legendre, L., Le Fèvre, J., 1989. Hydrodynamical singularities as controls of recycled versus export production in oceans. In: Berger, W.H., Smetacek, V.S., Wefer, G. (Eds.), Productivity of the Ocean, Present and Past. Wiley, Dahlem, pp. 49–63.

Li, W.K.W., 1994. Phytoplankton biomass and chlorophyll concentration across the North Atlantic. In: Rodríguez, J., Li, W.K.W. (Eds.), The Size Structure and Metabolism of the Pelagic Ecosystem. Scientia Marina, vol. 58, pp. 67–79.

Li, W.K.W., Wood, A.M., 1988. Vertical distribution of North Atlantic ultraphytoplankton: analysis by flow cytometry and epifluorescence microscopy. Deep-Sea Research 35, 1615–1638.

Longhurst, A., Harrison, W.G., 1989. The biological pump: Profiles of plankton production and consumption in the upper ocean. Progress in Oceanography 22, 47–123.

Malone, T.C., 1971. The relative importance of nanoplankton and netplankton as primary producers in tropical oceanic and neritic phytoplankton communities. Limnololgy and Oceanography 16, 633–639.

Malone, T.C., 1980. Algal size. In: Morris, Y. (Ed.), The Physiological Ecology of Phytoplankton. Blackwell, Oxford, pp. 433–454.

Mann, K.H., Lazier, J.R.N., 1991. Dynamics of Marine Ecosystems. Blackwell Scientific Publications, Oxford, 466 pp.

Margalef, R., 1978. Life-forms of phytoplankton as survival alternatives in an unstable environment. Oceanologica Acta 1, 493–509.

Parrilla, G., Kinder, T.H., 1987. Oceanografía física del Mar de Alborán. Boletín del Instituto Español de Oceanografía 4, 133–165.

Peña, M.A., Lewis, M.R., Harrison, G., 1990. Primary productivity and size structure of phytoplankton biomass on a transect of the equator at 135° W in the Pacific Ocean. Deep-Sea Research 37, 295–315.

Platt, T., Denman, K.L., 1977. Organisation in the pelagic ecosystem. Helgolander wissenschaftliche Meeresuntersuchungen 30, 575–581.

Platt, T., Denman, K.L., 1978. The structure of pelagic marine ecosystems. Rapports et Procès-Verbaux des Réunions du Conseil Internationale Pour l'Exploration Scientifique de la Mer. 173, 60–65.

Platt, T., Lewis, M., Geider, R., 1984. Thermodynamics of the pelagic ecosystem: Elementary closure conditions for biological production in the open ocean. In: Fasham, M.J.R. (Ed.), Flows of Energy and Material in Marine Ecosystem: Theory and Practice. NATO Conference Series IV, Marine Sciences, vol. 13. Plenum Press, New York, pp. 49–84.

Platt, T., Subba rao, D.V., Irwin, B., 1983. Photosynthesis of picoplankton in the oligotrophic ocean. Nature 301, 702–704.

Rodríguez, J., 1994. Some comments on the size-based structural analysis of the pelagic ecosystem. In: Rodríguez, J., Li, W.K.W. (Eds.), The Size Structure and Metabolism of the Pelagic Ecosystem. Scientia Marina vol. 58, pp. 1–10.

Rodríguez, J., Mullin, M.M., 1986. Relation between biomass and body weight of plankton in a steady state oceanic ecosystem. Limnology and Oceanography 31, 361–370.

Rodríguez, V., Guerrero, F., 1994. Chlorophyll a of size fractionated summer phytoplankton biomass at a coastal station in Málaga Bay, Alborán Sea. Estuarine, Coastal and Shelf Science 39, 413–419.

Ruíz, J., García, C.M., Rodríguez, J., 1996. Vertical patterns of phytoplankton size distribution in the Cantabric and Balearic seas. Journal of Marine Systems 9, 269–282.

Sieburth, J. McN., Smetacek, V., Lenz, J., 1978. Pelagic ecosystem structure: heterotrophic compartments of the plankton and their relationship to plankton size fractions. Limnology and Oceanography 23, 1256–1263.

Sheldon, R.W., Prakash, A., Sutcliffe Jr., W.H., 1972. The size distribution of particles in the ocean. Limnology and Oceanography 17, 327–340.

Sokal, R.R., Rohlf, F.J., 1985. Biometry, 3rd ed. Freeman, New York, 887 pp.

Sprules, W.G., Munawar, M., 1986. Plankton size spectra in relation to ecosystem productivity, size, and perturbation. Canadian Journal of Fisheries and Aquatic Sciences 43, 1789–1794.

Takahashi, M., Bienfang, P.K., 1983. Size structure of phytoplankton biomass and photosynthesis in subtropical Hawaiian waters. Marine Biology 76, 203–211.

Tintoré, J., Gomis, D., Alonso, S., Parrilla, G., 1991. Mesoscale dynamics and vertical motion in the Alborán Sea. Journal of Physical Oceanography 21, 811–823.

Varela, R.A., Cruzado, A., Tintoré, J., 1994. A simulation analysis of various biological and physical factors influencing the deep-chlorophyll maximum structure in oligotrophics areas. Journal of Marine Systems 5, 143–157.

Varela, R.A., Cruzado, A., Tintoré, J., Garcia-Ladona, E., 1992. Modelling the deep-chlorophyll maximum: a couppled physical- biological approach. Journal of Marine Research 50, 441–463.

Vaulot, D., Courties, C., Partensky, F., 1989. A simple method to preserve oceanic phytoplankton for flow cytometric analyses. In: Yentsch, C.M., Horan, P.K. (Eds.), Cytometry in Aquatic Sciences. Cytometry 10, pp. 629–635.

Venrick, E.L., McGowan, J.A., Mantyla, A.W., 1973. Deep chlorophyll maximun of photosynthetic chlorophyll in the Pacific Ocean. Fisheries Bulletin 71, 41–52.